Progress In Electromagnetics Research M, Vol. 45, 143–151, 2016

Fast Algorithm of Multi-region MoM-PO for Antennas on Electrically Large Platform

Bo Zhao*, Shu-Xi Gong, Xing Wang, and Yu Zhang

Abstract—For the radiation problem of multi-antenna on electrical-large platform, a multi-region MoM-PO (Multi-MoM-PO) is firstly proposed in this paper. The conventional MoM-PO generally treats all the antennas as a whole MoM region, but in the Multi-MoM-PO, each antenna is classified as one MoM region. On the basis of the mutual interaction between each MoM region and PO region, the self-interactions among MoM regions are considered. Numerical examples demonstrate that the multi-region technique can effectively boost the efficiency of impedance matrix filling compared with the conventional MoM-PO. Finally, the dependence of the filling efficiency against the number of antennas on platform is discussed.

1. INTRODUCTION

The radiation of antenna on electrical-large platform is an important task in the fields of electromagnetic compatibility (EMC) [1, 2] and antenna design. For this kind of problem, the hybrid method [3, 4], such as the MoM-PO [5–7], has proven to be an effective tool.

In the conventional MoM-PO [8, 9], the radiation system is divided into MoM region and PO region. Customarily, the antenna with its vicinity and the rest area fall into the MoM region and PO region, respectively. In essence, the influence of the platform on the antenna results from the radiation of antenna. So only the self-coupling of the MoM region and mutual coupling between the MoM and PO regions are taken into account. Therefore, the total number of the unknowns can be cut down to a large extent compared with the MoM. Correspondingly, the requirement of computer memory is greatly alleviated, and the solution time of the matrix equation is shortened drastically. On the other hand, the MoM region where the electrical currents densely exist is resolved by the MoM with high accuracy. Thus, the precision of the MoM-PO can be guaranteed.

In the previous literatures, it is rare to see the radiation analysis of multi-antenna on large platform. This is due to the fact that the conventional MoM-PO [8, 9] is not directly related with the number of antennas since all the antennas are seen equivalently as just one from a mathematical point of view. In this case, it is necessary to consider the coupling between the whole MoM region and PO region, which is the most time-consuming part of the total computation. Comparatively, the coupling computation will be greatly reduced provided that each antenna is defined as one MoM region and that each MoM region is coupling with the PO region. The more the number of antennas is, the more the coupling computation can be saved.

This idea of partitioning of the MoM region based on the MoM-PO is firstly applied to the analysis of multi-antenna on large-scale platform. The basic principle of Multi-MoM-PO and detailed presentation of formulae are given in Section 2. In Section 3, numerical results are displayed. Section 4 summarizes the contents of the paper.

Received 23 November 2015, Accepted 21 December 2015, Scheduled 3 January 2016
* Corresponding author: Bo Zhao (m15991342657@163.com).
The authors are with the National Key Laboratory of Antennas and Microwave Technology, Xidian University, Xi'an, Shaanxi 710071, China.

2. FORMULATION

2.1. A Brief Overview of the Conventional MoM-PO

The coupling electrical field integral equation (CEFIE) which is utilized to describe the system of antenna mounted on platform is given as,

$$\mathbf{E}^{inc}\big|_{\tan} = \left(L^E\mathbf{J}^{\mathrm{MoM}} + L^E\mathbf{J}^{\mathrm{PO}}\right)\big|_{\tan} \tag{1}$$

where $\mathbf{E}^{inc}$ is the electrical component of the incident plane wave; $\mathbf{J}^{\mathrm{MoM}}$ and $\mathbf{J}^{\mathrm{PO}}$ are the electrical currents in the MoM region and PO region, respectively; L^E denotes the operator concerned with the electrical field integral equation (EFIE).

$$\mathbf{J}^{\mathrm{MoM}} = \sum_{n=1}^{N_{\mathrm{MoM}}} I_n^{\mathrm{MoM}}\mathbf{f}_n^{\mathrm{MoM}} \tag{2}$$

$$\mathbf{J}^{\mathrm{PO}} = \sum_{k=1}^{N_{\mathrm{PO}}} I_k^{\mathrm{PO}}\mathbf{f}_k^{\mathrm{PO}} \tag{3}$$

$$L^E\mathbf{J} = jk\eta\int_s\left[\mathbf{J}\left(\mathbf{r}'\right) + \frac{1}{k^2}\nabla\nabla'\cdot\mathbf{J}\left(\mathbf{r}'\right)\right]G\left(\mathbf{r},\mathbf{r}'\right)ds' \tag{4}$$

where $\mathbf{f}_n^{\mathrm{MoM}}$ and $\mathbf{f}_k^{\mathrm{PO}}$ indicate the RWG basis function [10, 11] of $\mathbf{J}^{\mathrm{MoM}}$ and $\mathbf{J}^{\mathrm{PO}}$; N_{MoM} and N_{MoM} correspond to the number of $\mathbf{f}_n^{\mathrm{MoM}}$ and $\mathbf{f}_k^{\mathrm{PO}}$; I_n^{MoM} and I_k^{PO} are the expansion coefficients of $\mathbf{f}_n^{\mathrm{MoM}}$ and $\mathbf{f}_k^{\mathrm{PO}}$; k, η, and G are the wavenumber, wave impedance, and Green function in free space, respectively. Following the substitution of Eqs. (2)–(4) into Eq. (1) and the Galerkin testing procedure, Eq. (1) can be changed to Eq. (5),

$$\sum_{n=1}^{N_{\mathrm{MoM}}} I_n^{\mathrm{MoM}}\left\langle\mathbf{f}_m, L^E\mathbf{f}_n^{\mathrm{MoM}}\right\rangle + \sum_{k=1}^{N_{\mathrm{PO}}} I_k^{\mathrm{PO}}\left\langle\mathbf{f}_m, L^E\mathbf{f}_k^{\mathrm{PO}}\right\rangle = \left\langle\mathbf{f}_m, \mathbf{E}^i\right\rangle, \quad m = 1, 2, \ldots, N_{\mathrm{MoM}} \tag{5}$$

The matrix form of Eq. (5) can be written as,

$$\left[Z_{m,n}^{\mathrm{MoM}} + Z_{m,n}^{\mathrm{PO}}\right]\left[I_n^{\mathrm{MoM}}\right] = \left[V_m^{\mathrm{MoM}}\right], \quad m, n = 1, 2, \ldots, N_{\mathrm{MoM}} \tag{6}$$

where $[Z_{m,n}^{\mathrm{MoM}}]$ is the self-impedance matrix of the MoM region, $[Z_{m,n}^{\mathrm{PO}}]$ the coupling impedance matrix between the MoM and PO regions, $[V_m^{\mathrm{MoM}}]$ the excitation vector, and $[I_n^{\mathrm{MoM}}]$ the coefficient vector of electrical current.

To facilitate the following description, the expression of elements of the coupling matrix $[Z_{m,n}^{\mathrm{PO}}]$ is deduced as follow. Firstly, a pair of unit vectors, $\hat{\mathbf{t}}_k^+$ and $\hat{\mathbf{t}}_k^-$ [8, 9], defined on the RWG basis function is introduced. Combining with Eq. (3), I_k^{PO} can be rearranged as below,

$$I_k^{\mathrm{PO}} = \frac{1}{2}\left(\hat{\mathbf{t}}_k^+ + \hat{\mathbf{t}}_k^-\right)\cdot\mathbf{J}^{\mathrm{PO}} \tag{7}$$

According to the PO theory, the electrical currents in the PO region are obtained as,

$$\mathbf{J}^{\mathrm{PO}} = 2\delta_{J,n}\hat{\mathbf{n}}\times L^H\mathbf{J}^{\mathrm{MoM}} \tag{8}$$

where $\delta_{J,n}$ is the shadowing effect coefficient [12], $\hat{\mathbf{n}}$ the unit normal vector in the PO region, and L^H the operator resulting from the magnetic field integral equation (MFIE) and can be written as,

$$L^H\mathbf{J} = \nabla\times\int_S\mathbf{J}\left(\mathbf{r}'\right)G\left(\mathbf{r},\mathbf{r}'\right)ds' \tag{9}$$

Combined with Eqs. (3), (7) and (8), the second term on the left side of equal sign in Eq. (5) can be expressed as,

$$\sum_{n=1}^{N_{\mathrm{MoM}}} I_n^{\mathrm{MoM}}\left[\sum_{k=1}^{N_{\mathrm{PO}}}\delta_{J,n}\left(\hat{\mathbf{t}}_k^+ + \hat{\mathbf{t}}_k^-\right)\cdot\left(\hat{\mathbf{n}}\times L^H\mathbf{f}_n^{\mathrm{MoM}}\right)\left\langle\mathbf{f}_m, L^E\mathbf{f}_k^{\mathrm{PO}}\right\rangle\right], \quad m = 1, 2, \ldots, N_{\mathrm{MoM}} \tag{10}$$

Comparing Eq. (10) with the term $[Z_{m,n}^{\mathrm{PO}}]\,[I_n^{\mathrm{MoM}}]$ in Eq. (6), the elements of $[Z_{m,n}^{\mathrm{PO}}]$ are concluded below,

$$Z_{m,n}^{\mathrm{PO}} = \sum_{k=1}^{N_{\mathrm{PO}}} \delta_{J,n} \left(\hat{\mathbf{t}}_k^{+} + \hat{\mathbf{t}}_k^{-}\right) \cdot \left(\hat{\mathbf{n}} \times L^H \mathbf{f}_n^{\mathrm{MoM}}\right) \left\langle \mathbf{f}_m, L^E \mathbf{f}_k^{\mathrm{PO}} \right\rangle \tag{11}$$

2.2. The Multi-MoM-PO

The number of antennas on platform is assumed to be x. In the conventional MoM-PO, all the antennas are classified as unique MoM region, and Eq. (5) or (6) is employed to get $\mathbf{J}^{\mathrm{MoM}}$. However, if we regard each antenna as one MoM region, as shown in Fig. 1, the electrical currents expanded by RWG basis functions corresponding to the x MoM regions are listed below,

$$\begin{cases} \mathbf{J}^{\mathrm{MoM1}} = \sum\limits_{n1=1}^{N1} I_{n1}^{\mathrm{MoM1}} \mathbf{f}_{n1}^{\mathrm{MoM1}} \\ \mathbf{J}^{\mathrm{MoM2}} = \sum\limits_{n2=1}^{N2} I_{n2}^{\mathrm{MoM2}} \mathbf{f}_{n2}^{\mathrm{MoM2}} \\ \cdots \\ \mathbf{J}^{\mathrm{MoM}x} = \sum\limits_{nx=1}^{Nx} I_{nx}^{\mathrm{MoM}x} \mathbf{f}_{nx}^{\mathrm{MoM}x} \end{cases} \tag{12}$$

where $\mathbf{J}^{\mathrm{MoM}i}$ and $\mathbf{f}_{ni}^{\mathrm{MoM}i}$, $i = 1, 2, \ldots, x$ are the electrical current and RWG basis function in the ith MoM region; Ni is the number of RWG basis functions used to expand $\mathbf{J}^{\mathrm{MoM}i}$; $I_{ni}^{\mathrm{MoM}i}$ is the coefficient of $\mathbf{J}^{\mathrm{MoM}i}$ expanded by $\mathbf{f}_{ni}^{\mathrm{MoM}i}$. Under this circumstance, the mutual interaction between MoM and PO regions is accounted for and then the self-interaction among the MoM regions should be considered on the whole. This procedure is displayed in the equation below.

$$\begin{bmatrix} \left[Z_{m1,n1}^{\mathrm{MoM11}} + Z_{m1,n1}^{\mathrm{PO1}}\right] & \left[Z_{m1,n2}^{\mathrm{MoM12}}\right] & \cdots & \left[Z_{m1,nx}^{\mathrm{MoM1}x}\right] \\ \left[Z_{m2,n1}^{\mathrm{MoM21}}\right] & \left[Z_{m2,n2}^{\mathrm{MoM22}} + Z_{m2,n2}^{\mathrm{PO2}}\right] & \cdots & \left[Z_{m2,nx}^{\mathrm{MoM1}x}\right] \\ \vdots & \vdots & \ddots & \vdots \\ \left[Z_{mx,n1}^{\mathrm{MoM}x2}\right] & \left[Z_{mx,n2}^{\mathrm{MoM}x2}\right] & \cdots & \left[Z_{mx,nx}^{\mathrm{MoM}xx} + Z_{mx,nx}^{\mathrm{PO}x}\right] \end{bmatrix} \begin{bmatrix} \left[I_{n1}^{\mathrm{MoM1}}\right] \\ \left[I_{n2}^{\mathrm{MoM2}}\right] \\ \vdots \\ \left[I_{nx}^{\mathrm{MoM}x}\right] \end{bmatrix} = \begin{bmatrix} \left[V_{m1}^{\mathrm{MoM1}}\right] \\ \left[V_{m2}^{\mathrm{MoM2}}\right] \\ \vdots \\ \left[V_{mx}^{\mathrm{MoM}x}\right] \end{bmatrix} \tag{13}$$

In Eq. (13), $[Z_{mi,ni}^{\mathrm{MoM}ii}]$ is the impedance submatrix due to the ith MoM region and means the self-interaction of the ith antenna; $[Z_{mi,ni}^{\mathrm{PO}i}]$ is the corrected impedance submatrix which represents the

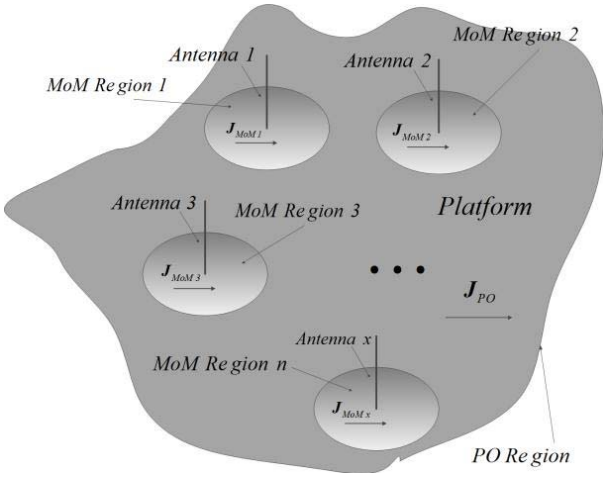

Figure 1. Model of Multi-MoM-PO.

mutual interaction between the ith MoM region and PO region or between the ith antenna and the large platform. The calculation of elements of the corrected impedance submatrix conforms to Eq. (11). $[Z_{mi,nj}^{\mathrm{MoM}ij}]$ is the mutual interaction submatrix of the MoM regions between the ith antenna and the jth antenna; $[V_{mi}^{\mathrm{MoM}i}]$ is the excitation vector due to the feeding of the ith antennas and $[I_{ni}^{\mathrm{MoM}i}]$ the coefficient vector of electrical currents of the ith antenna on platform.

It can be seen from Eq. (6) that the conventional MoM-PO does not possess the characteristic of block submatrices. Therefore, all the elements of impedance matrix have to be corrected by $Z_{m,n}^{\mathrm{PO}}$. By contrast, it is clear to see in Eq. (13) that only the elements of the diagonal block submatrices should be modified. In other words, the number of the submatrices requiring modification in the Multi-MoM-PO is x while that in the conventional MoM-PO is x^2 equivalently. Further, with the increase of the number of antennas, the advantage of the Multi-MoM-PO will be more evident. In addition, it should be noted that in the implemented codes, the filling of submatrix $[Z_{mi,ni}^{\mathrm{MoM}ii}]$ or $[Z_{mi,nj}^{\mathrm{MoM}ij}]$ means double loop while that of $[Z_{mi,ni}^{\mathrm{PO}i}]$ triplet loop. Hence, the computational complexity of $[Z_{mi,ni}^{\mathrm{PO}i}]$ is much greater than that of $[Z_{mi,ni}^{\mathrm{MoM}ii}]$ or $[Z_{mi,nj}^{\mathrm{MoM}ij}]$ with the same size. In conclusion, the computational complexity of the impedance matrix filling of the Multi-MoM-PO is approximately $1/x$ as that of the conventional MoM-PO.

When Eqs. (6) and (13) are compared, a question will occur: why the same electrical current vector is obtained on the occasion that the serial number of antennas and distribution of the unknowns belonging to anyone of the antennas stay consistent with each other. Further analysis indicates that although the two impedance matrices are different, the two excitation vectors are not the same correspondingly. Consequently, it is possible that the solutions of Eqs. (6) and (13) are the same, which will be demonstrated in the subsequent section.

3. NUMERICAL RESULTS AND DISCUSSION

This section presents three numerical examples to testify the efficiency and accuracy of the proposed technique in this paper. All the antennas radiate at 300 MHz and adopt the delta-gap feeding. The program codes of Fortran are implemented on a 2.0 GHz workstation with 32G memory. The mesh size in the MoM region ranges from 0.1λ to 0.125λ while that in PO region is 0.3λ. To clearly display the calculation process, each numerical example is followed by a table of time information. The total CPU time is decomposed into the pre-processing time, matrix filling time, solution time, and post-processing time. It should be noted that the judgement of shadowing effect coefficients is performed independently and is not included in the pre-processing time.

3.1. Two Monopoles Mounted on a Partial Sphere

In the first example, we consider two monopoles mounted on a platform of a partial sphere. The configuration and physical dimension of the radiation system are shown in Fig. 2. The two antennas

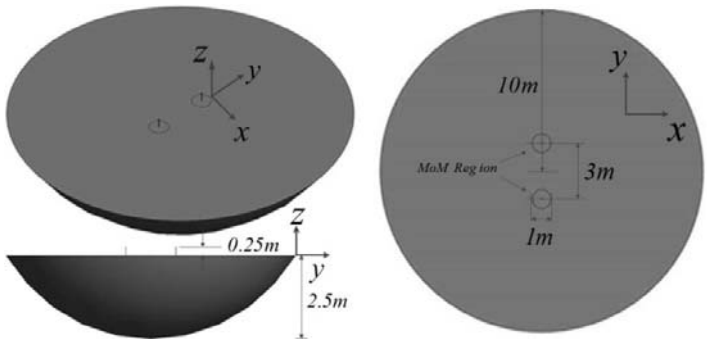

Figure 2. Two monopoles on a partial sphere.

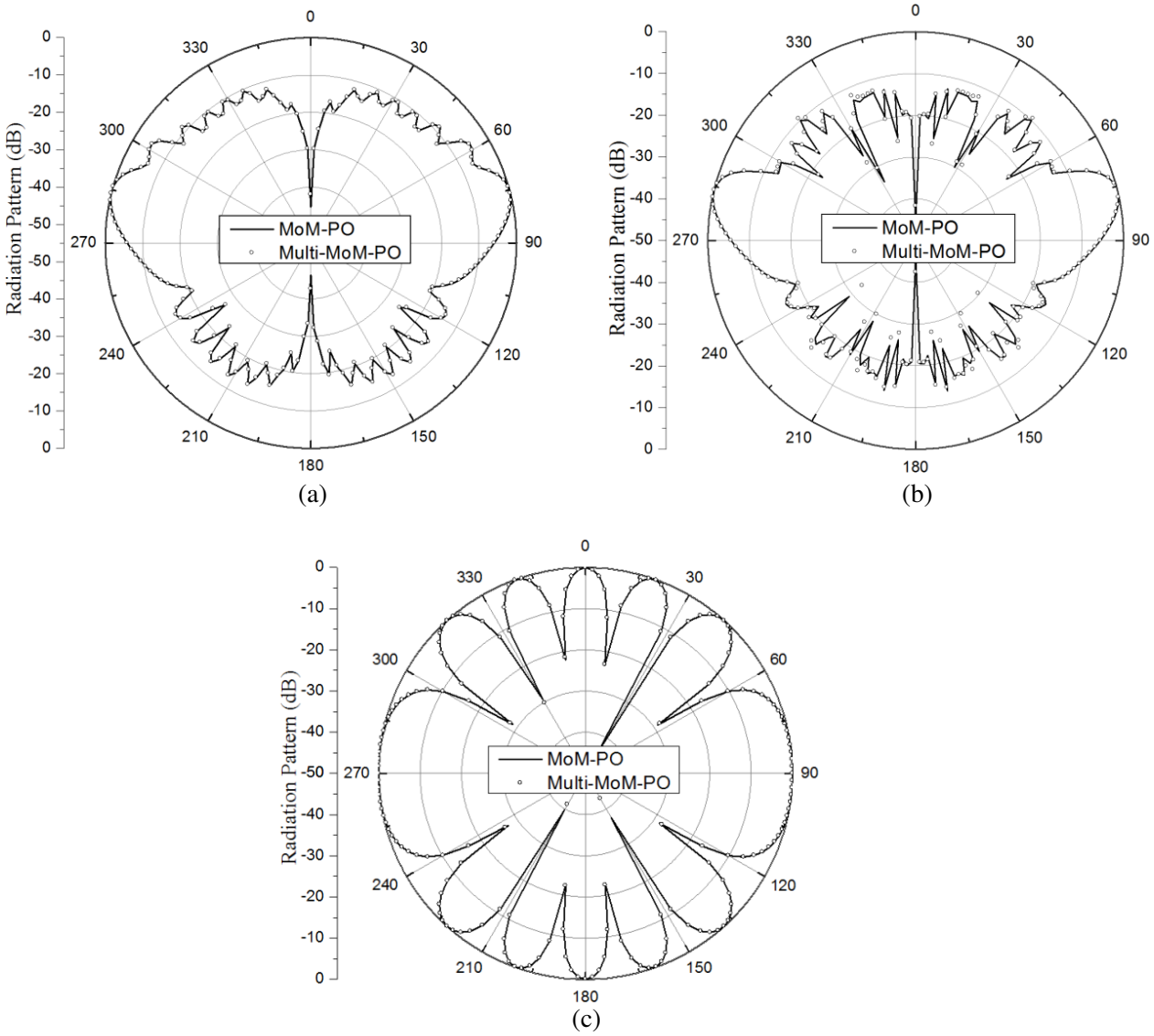

Figure 3. Radiation patterns in the (a) XoZ, (b) YoZ, and (c) XoY planes of two monopoles mounted on a partial sphere.

Table 1. Detailed information of CPU time of examples 1.

Method	Pre-process	Matrix filling	Solution	Post-process	Total CPU time
MoM-PO	8.0	67617.7	22.4	22.5	67670.5
Multi-MoM-PO	7.8	33978.6	20.4	19.5	34026.3

with their surrounding circular areas are defined as the MoM region while the rest surface the PO region. The MoM region is meshed into 398 triangles corresponding to 552 unknowns. And the PO region is discretized into 19184 triangles and 28741 unknowns. Fig. 3 shows the radiation patterns of three cut-planes obtained from the conventional MoM-PO and Multi-MoM-PO. It can be seen from this figure that the solution of the Multi-MoM-PO is in good agreement with that of the conventional MoM-PO. Table 1 lists the computation time at each stage. Evidently, the matrix filling time occupies the dominant part of the total CPU time. The matrix filling time of MoM-PO is 1.99 times as that of Multi-MoM-PO, which conforms to the prediction of computational complexity at the end of Section 2.

Table 2. Detailed information of CPU time of examples 2.

Method	Pre-process	Matrix filling	Solution	Post-process	Total CPU time
MoM-PO	102.5	31179.1	35.1	95.3	31412.1
Multi-MoM-PO	103.0	8568.4	26.1	69.9	8767.4

3.2. Three Monopoles Installed on the Top of an Airplane

In the second example, three monopoles are installed on the top of an airplane. The detailed dimensions and antenna layout are displayed in Fig. 4. The MoM region consists of three monopoles and their bases while the remainder belongs to the PO region. The MoM and PO regions are discretized into 138 and 68972 triangles which lead to 177 and 103434 unknowns, respectively. The normalized radiation patterns in XOZ, YOZ, and XOY planes are exhibited in Fig. 5. It is clear to see that the results of the Multi-MoM-PO are consistent with that of the conventional MoM-PO. From Table 2, it can be seen that the ratio of matrix filling time to the total CPU time is 99.3% in MoM-PO and 97.7% in Multi-MoM-PO. The matrix filling time of MoM-PO is 3.64 times of that of Multi-MoM-PO.

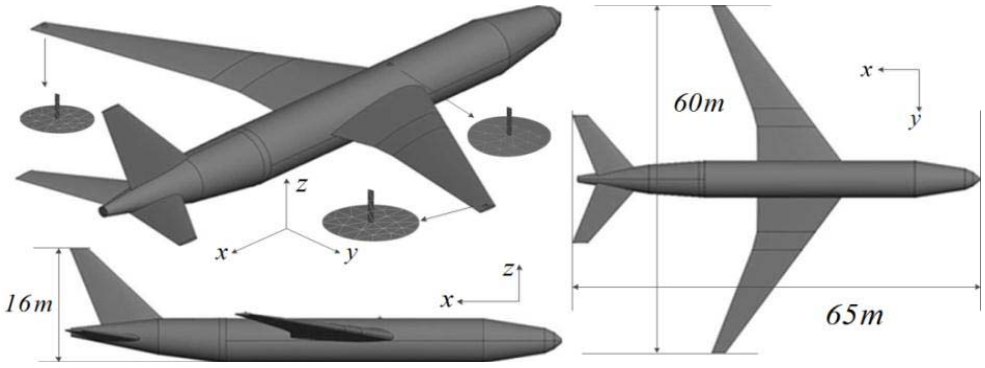

Figure 4. Three monopoles installed on the top of an airplane.

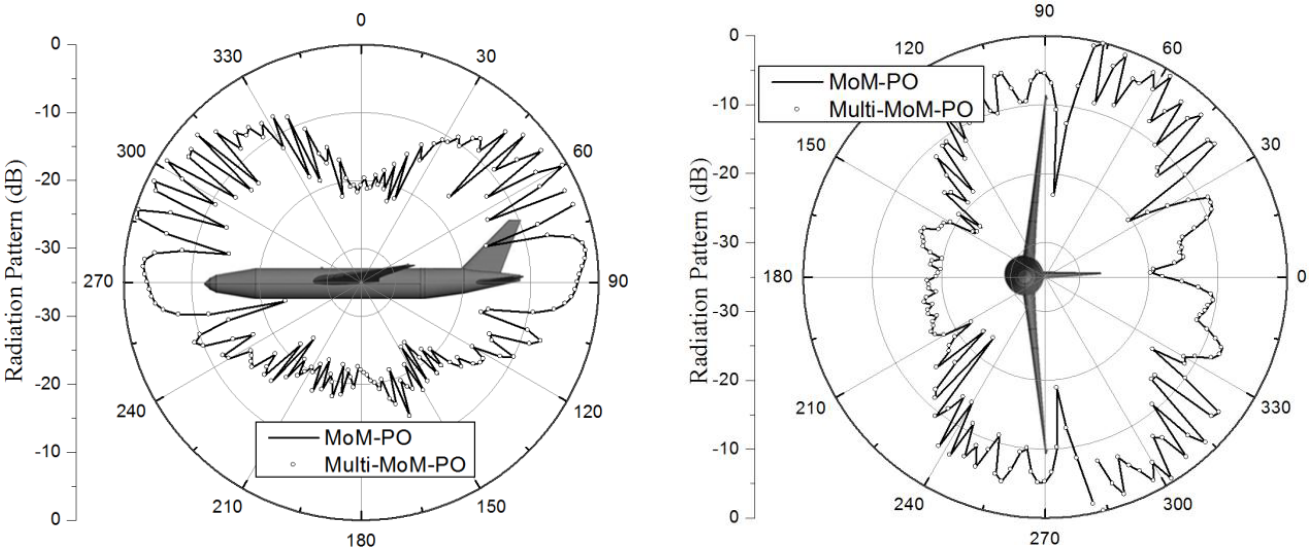

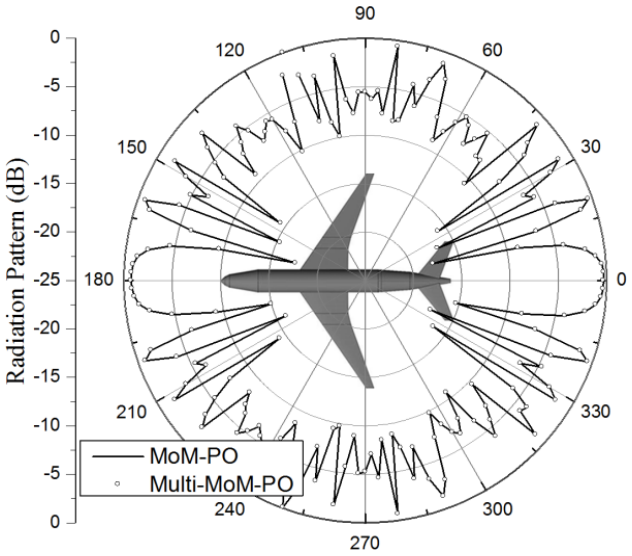

(c)

Figure 5. Radiation patterns in the (a) XoZ, (b) YoZ, and (c) XoY planes of three monopoles installed on the top of an airplane.

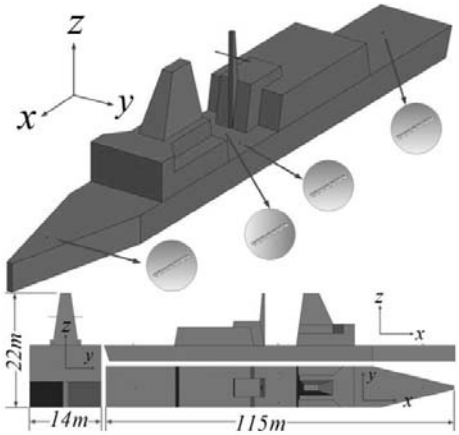

Figure 6. Four dipoles around a ship.

3.3. Four Dipoles around a Ship

In the last example, the model includes four dipoles around a ship, and all the dipoles are 0.5 m above the deck, as shown in Fig. 6. The dipoles and ship are classified into the MoM and PO regions which are discretized into 48 and 175421 triangles. Correspondingly, there are 44 and 263178 RWG basis functions belonging to the MoM and PO regions, respectively. The normalized radiation patterns in XOZ, YOZ, XOY planes are manifested in Fig. 7. Good agreement is also obtained between the consequences of the Multi-MoM-PO and conventional MoM-PO. The pre-processing time, matrix filling time, solution

Table 3. Detailed information of CPU time of examples 3.

Method	Pre-process	Matrix filling	Solution	Post-process	Total CPU time
MoM-PO	787.1	4666.3	19.1	211.1	5683.6
Multi-MoM-PO	787.2	1110.4	18.5	194.5	2110.7

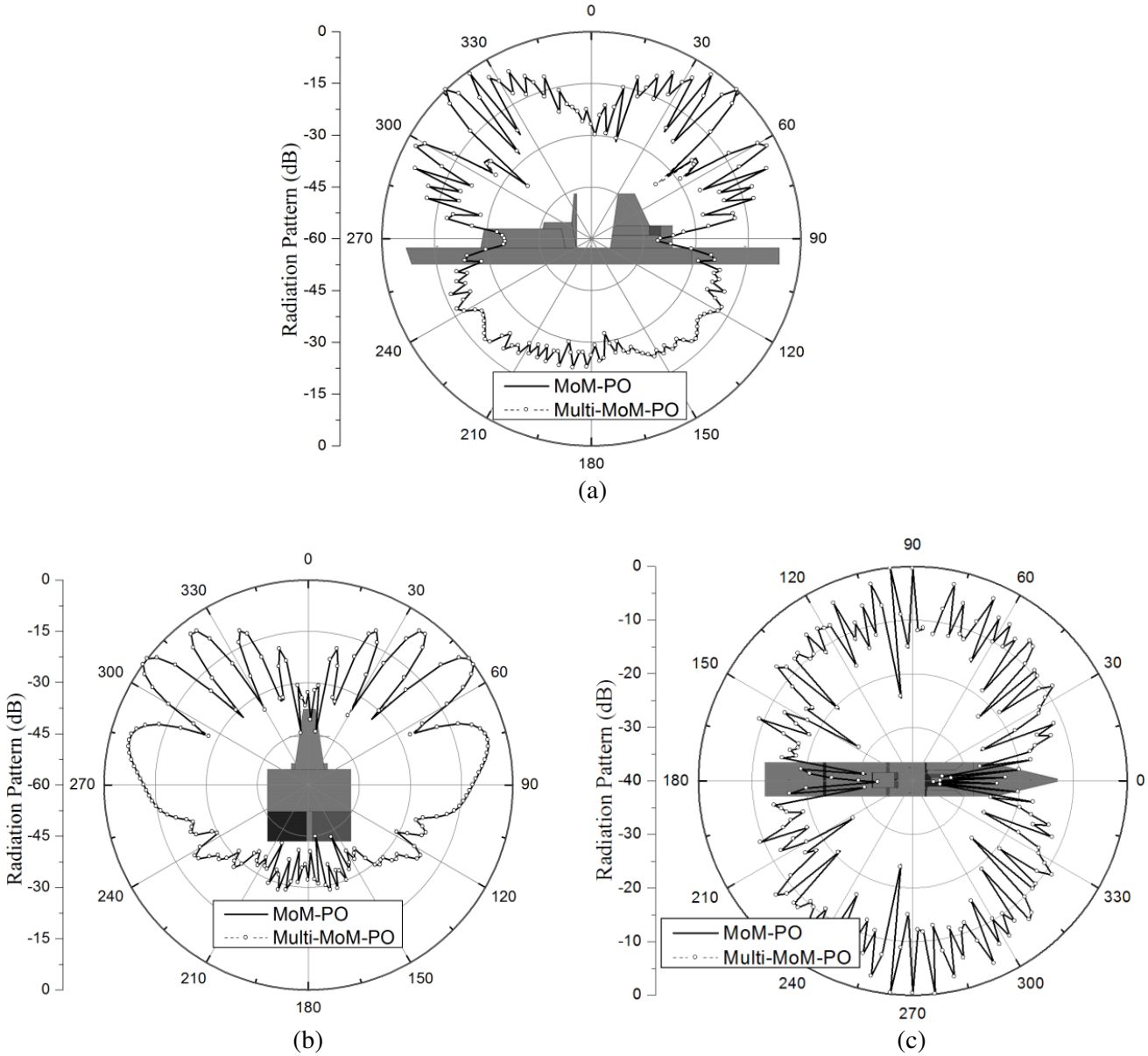

Figure 7. Radiation patterns in the (a) XoZ, (b) YoZ, and (c) XoY planes of four dipoles around a ship.

time, post-processing time and total CPU time are organized in Table 3. The time ratio of matrix filling of MoM-PO to Multi-MoM-PO is 4.20 which meets the conclusion at the end of Section 2 well.

4. CONCLUSION

The efficient Multi-MoM-PO has been proposed in this paper for computing radiation problem of multi-antenna in the presence of large-scale platform. A brief review of the conventional MoM-PO is presented, and the formula of the corrected element of the impedance matrix is deduced. Then the Multi-MoM-PO is described in the form of matrix, and its computational complexity is revealed. Numerical examples illustrate that compared with the conventional MoM-PO, efficient filling of matrix can be achieved by the proposed technique which is especially suitable for the analysis of multi-antenna on platform.

ACKNOWLEDGMENT

This work is supported by the National High Technology Research and Development Program of China (863 Program) (No. 2012AA01A308), the National Natural Science Foundation of China (Nos. 61401327, 61201018, 61471278, 61501343), the Program for New Century Excellent Talents in University of China (No. NCET-13-0949), Shaanxi Youth Science and Technology Star Project (No. 2013KJXX-67).

REFERENCES

1. Wei, X. C. and E. P. Li, "Wide-band EMC analysis of on-platform antennas using impedance-matrix interpolation with the moment method-physical optics method," *IEEE Trans. Electromagn. Compat.*, Vol. 45, No. 3, 552–556, Aug. 2003.
2. Lei, J.-Z., C.-H. Liang, W. Ding, and Y. Zhang, "EMC analysis of antennas mounted on electrically large platforms with parallel FDTD method," *Progress In Electromagnetics Research*, Vol. 84, 205–220, 2008.
3. Davidson, S. A. and G. A. Thiele, "A hybrid method of moments-GTD technique for computing electromagnetic coupling between two monopole antennas on a large cylindrical surface," *IEEE Trans. Electromagn. Compat.*, Vol. 26, No. 2, 90–97, May 1984.
4. Thiele, G. A., "Overview of selected hybrid methods in radiating system analysis," *Proc. IEEE*, Vol. 80, No. 1, 66–78, Jan. 1992.
5. Zhao, X.-W., Y. Zhang, H.-W. Zhang, D. Garcia-Donoro, S.-W. Ting, T. K. Sarkar, and C.-H. Liang, "Parallel MoM-PO method with out-of-core technique for analysis of complex arrays on electrically large platforms," *Progress In Electromagnetics Research*, Vol. 108, 1–21, 2010.
6. Ma, J., S.-X. Gong, X. Wang, Y.-X. Xu, W.-J. Zhao, and J. Ling, "Efficient IE-FFT and PO hybrid analysis of antennas around electrically large platforms," *IEEE Antennas Wireless Propag. Lett.*, Vol. 10, 611–614, 2011.
7. Wang, X., S.-X. Gong, J. Ma, and C.-F. Wang, "Efficient analysis of antennas mounted on large-scale complex platforms using hybrid AIM-PO technique," *IEEE Trans. Antennas Propag.*, Vol. 62, No. 3, 1517–1523, Mar. 2014.
8. Jakobus, U. and F. M. Landstorfer, "Improved PO-MM hybrid formulation for scattering from three-dimensional perfectly conducting bodies of arbitrary shape," *IEEE Trans. Antennas Propag.*, Vol. 43, No. 2, 162–169, Feb. 1995.
9. Ma, J., S.-X. Gong, X. Wang, Y. Liu, and Y.-X. Xu, "Efficient wide-band analysis of antennas around a conducting platform using MoM-PO hybrid method and asymptotic waveform evaluation technique," *IEEE Trans. Antennas Propag.*, Vol. 62, No. 12, 6048–6052, Dec. 2012.
10. Rao, S. M., D. R. Wilton, and A. W. Glisson, "Electromagnetic scattering by surfaces of arbitrary shape," *IEEE Trans. Antennas Propag.*, Vol. 30, No. 3, 409–418, May 1982.
11. Ylä-Oijala, P., J. Markkanen, S. Järvenpää, and S. P. Kiminki, "Surface and volume integral equation methods for time-harmonic solutions of Maxwell's equations," *Progress In Electromagnetics Research*, Vol. 149, 15–44, 2014.
12. Zhao, W.-J., L.-W. Li, and L. Hu, "Efficient current-based hybrid analysis of wire antennas mounted on a large realistic aircraft," *IEEE Trans. Antennas Propag.*, Vol. 58, No. 8, 2666–2672, Aug. 2010.